Contamination of the Accuracy of the Surface Integral Equations with the Discretization Error of the Identity Operator

Özgür Ergül[1,2] **and Levent Gürel**[1,2]
[1]Department of Electrical and Electronics Engineering
[2]Computational Electromagnetics Research Center (BiLCEM)
Bilkent University, TR-06800, Bilkent, Ankara, Turkey
E-mail: ergul@ee.bilkent.edu.tr, lgurel@bilkent.edu.tr

Abstract — We consider the solution of electromagnetics problems formulated with surface integral equations (SIE) and discretized with low-order basis functions, such as the Rao-Wilton-Glisson functions. Normal and mixed SIE formulations involving well-tested identity operators are significantly inaccurate compared to tangential formulations. We show that the well-tested identity operator is a major error source that contaminates the accuracy of SIE formulations. Due to excessive discretization error of the identity operator, matrix equations obtained with tangential, normal, and mixed formulations are incompatible. We also show that, in an iterative solution of a normal or mixed formulation, the minimization of the residual error involves a breakpoint, where a further reduction of the residual error does not improve the solution in terms of compatibility with the corresponding tangential formulation. This breakpoint corresponds to the last useful iteration, where the accuracy of the solution is saturated and a further reduction of the residual error is practically unnecessary.

1. INTRODUCTION

Surface integral equations (SIE) are commonly used for the solution of scattering and radiation problems in electromagnetics [1]. Complicated problems involving three-dimensional metallic and/or homogeneous dielectric structures are formulated rigorously by defining equivalent current on surfaces and applying the boundary conditions. Depending on the testing scheme and the boundary conditions used, there are four basic SIEs, namely, the tangential electric-field integral equation (T-EFIE), the normal electric-field integral equation (N-EFIE), the tangential magnetic-field integral equation (T-MFIE), and the normal magnetic-field integral equation (N-MFIE) [2]. Various SIE formulations can be derived by using diverse combinations of SIEs. For numerical solutions, those formulations are discretized by expanding the equivalent currents and using the method of moments. The resulting dense matrix equations can be solved iteratively by using a Krylov subspace algorithm, which can be accelerated via fast solvers, such as the multilevel fast multipole algorithm [3].

SIE formulations can be categorized into three groups, i.e., tangential, normal, and mixed formulations, depending on their contents. Tangential formulations involve T-EFIE and/or T-MFIE, while normal formulations involve N-EFIE and/or N-MFIE. Mixed formulations are obtained by combining tangential and normal formulations, and they contain at least one tangential equation (T-EFIE and T-MFIE) and one normal equation (N-EFIE and N-MFIE). Using a Galerkin scheme for the discretization, normal and mixed formulations contain well-tested identity operators. It is well-known that matrix equations involving well-tested identity operators are diagonally dominant and they are well-conditioned. Therefore, iterative solutions of normal and mixed formulations are usually more efficient than the solutions of tangential formulations, which do not contain well-tested identity operators. On the other hand, recent studies show that tangential formulations are significantly more accurate than normal

This work was supported by the Scientific and Technical Research Council of Turkey (TUBITAK) under Research Grants 105E172 and 107E136, by the Turkish Academy of Sciences in the framework of the Young Scientist Award Program (LG/TUBA-GEBIP/2002-1-12), and by contracts from ASELSAN and SSM.

and mixed formulations, especially when they are discretized with low-order basis functions [4]–[8], such as the Rao-Wilton-Glisson (RWG) functions [9]. Discrepancy between the results obtained with tangential, normal, and mixed formulations can be reduced by employing more appropriate, especially higher-order, basis functions [10]–[17]. Investigations on the accuracy of SIE formulations also show that the source of the error is the identity operator [5],[18],[19]. Specifically, regularization of the identity operator improves the accuracy of N-MFIE for metallic objects [5],[19].

In this paper, we investigate the contamination of the accuracy of SIEs with the excessive discretization error of the identity operator. By setting up a computational experiment based on nonradiating currents, we prove that the identity operator is truly a major error source in SIE formulations. Since the discretization of the identity operator contaminates the accuracy of normal and mixed formulations, matrix equations obtained with tangential, normal, and mixed formulations for the same problem are incompatible. Then, the iterative solution of a normal or mixed formulation involves a breakpoint, where the compatibility of the solution with the corresponding tangential formulation is saturated. We show that this breakpoint corresponds to the last useful iteration, where the accuracy of the solution cannot be improved anymore.

2. SURFACE INTEGRAL EQUATION FORMULATIONS

Consider a homogeneous domain D_u bounded by a closed surface S_u and that may extend to infinity. T-EFIE is derived by directly testing the boundary condition for the tangential electric field on the surface, i.e.,

$$\hat{\boldsymbol{t}} \cdot \left\{ \mathcal{T}_u\{\boldsymbol{J}\}(\boldsymbol{r}) - \eta_u^{-1}\mathcal{K}_u\{\boldsymbol{M}\}(\boldsymbol{r}) - \frac{\Omega_o(\boldsymbol{r})}{4\pi}\eta_u^{-1}\mathcal{I}^{\times n}\{\boldsymbol{M}\}(\boldsymbol{r}) \right\} = -\hat{\boldsymbol{t}} \cdot \eta_u^{-1}\boldsymbol{E}^{inc}(\boldsymbol{r}), \tag{1}$$

where $\Omega_o(\boldsymbol{r})$ is the external solid angle at the observation point $\boldsymbol{r} \in S_u$, $\hat{\boldsymbol{t}}$ is any tangential unit vector, $\boldsymbol{E}^{inc}(\boldsymbol{r})$ is the incident electric field produced by the external sources inside D_u, and $\eta_u = \sqrt{\mu_u/\epsilon_u}$ is the wave impedance. In (1), $\boldsymbol{J}(\boldsymbol{r}) = \hat{\boldsymbol{n}} \times \boldsymbol{H}(\boldsymbol{r})$ and $\boldsymbol{M}(\boldsymbol{r}) - \hat{\boldsymbol{n}} \times \boldsymbol{E}(\boldsymbol{r})$ are equivalent surface currents, where $\hat{\boldsymbol{n}}$ is the normal vector pointing into D_u. Operators are defined as

$$\mathcal{T}_u\{\boldsymbol{X}\}(\boldsymbol{r}) = ik_u \int_{S_u} d\boldsymbol{r'} \Big[\boldsymbol{X}(\boldsymbol{r'}) + \frac{1}{k_u^2}\nabla' \cdot \boldsymbol{X}(\boldsymbol{r'})\nabla \Big] g_u(\boldsymbol{r}, \boldsymbol{r'}) \tag{2}$$

$$\mathcal{K}_u\{\boldsymbol{X}\}(\boldsymbol{r}) = \int_{S_u, PV} d\boldsymbol{r'} \boldsymbol{X}(\boldsymbol{r'}) \times \nabla' g_u(\boldsymbol{r}, \boldsymbol{r'}) \tag{3}$$

$$\mathcal{I}^{\times n}\{\boldsymbol{X}\}(\boldsymbol{r}) = \hat{\boldsymbol{n}} \times \mathcal{I}\{\boldsymbol{X}\}(\boldsymbol{r}) = \hat{\boldsymbol{n}} \times \boldsymbol{X}(\boldsymbol{r}), \tag{4}$$

where PV indicates the principal value of the integral, $k_u = \omega\sqrt{\mu_u \epsilon_u}$ is the wavenumber, and $g_u(\boldsymbol{r}, \boldsymbol{r'})$ denotes the homogeneous-space Green's function defined as

$$g_u(\boldsymbol{r}, \boldsymbol{r'}) = \frac{\exp(ik_u R)}{4\pi R} \qquad \Big(R = |\boldsymbol{r} - \boldsymbol{r'}|\Big). \tag{5}$$

N-EFIE is derived similarly by testing the boundary condition for the electric field projected onto the surface via $\hat{\boldsymbol{n}}$, i.e.,

$$\hat{\boldsymbol{n}} \times \left\{ \mathcal{T}_u\{\boldsymbol{J}\}(\boldsymbol{r}) - \eta_u^{-1}\mathcal{K}_u\{\boldsymbol{M}\}(\boldsymbol{r}) - \frac{\Omega_o(\boldsymbol{r})}{4\pi}\eta_u^{-1}\mathcal{I}^{\times n}\{\boldsymbol{M}\}(\boldsymbol{r}) \right\} = -\hat{\boldsymbol{n}} \times \eta_u^{-1}\boldsymbol{E}^{inc}(\boldsymbol{r}). \tag{6}$$

Finally, T-MFIE and N-MFIE are derived by testing the boundary condition for the tangential magnetic field, i.e.,

$$\left\{ \begin{array}{c} \hat{\boldsymbol{t}}\cdot \\ \hat{\boldsymbol{n}}\times \end{array} \right\} \left\{ \mathcal{T}_u\{\boldsymbol{M}\}(\boldsymbol{r}) + \eta_u\mathcal{K}_u\{\boldsymbol{J}\}(\boldsymbol{r}) + \frac{\Omega_o(\boldsymbol{r})}{4\pi}\eta_u\mathcal{I}^{\times n}\{\boldsymbol{J}\}(\boldsymbol{r}) \right\} = -\left\{ \begin{array}{c} \hat{\boldsymbol{t}}\cdot \\ \hat{\boldsymbol{n}}\times \end{array} \right\} \eta_u \boldsymbol{H}^{inc}(\boldsymbol{r}), \tag{7}$$

where $\boldsymbol{H}^{inc}(\boldsymbol{r})$ is the incident magnetic field.

Table 1. Surface Integral Equation Formulations

Formulation	Integral Equation Content	Object Type
T-EFIE	T-EFIE	Metallic
N-MFIE	N-MFIE	Metallic
T-N-CFIE	T-EFIE+N-MFIE	Metallic
TN-N-CFIE	T-EFIE$_0$+N-EFIE$_0$+N-MFIE$_0$ T-EFIE$_I$+N-EFIE$_I$+N-MFIE$_I$	Dielectric
T-PMCHWT and CTF	T-EFIE$_0$+T-EFIE$_I$ T-MFIE$_0$+T-MFIE$_I$	Dielectric
NMF and MNMF	N-MFIE$_0$+N-MFIE$_I$ N-EFIE$_0$+N-EFIE$_I$	Dielectric
JMCFIE	T-EFIE$_0$+T-EFIE$_I$+N-MFIE$_0$+N-MFIE$_I$ T-MFIE$_0$+T-MFIE$_I$+ N-EFIE$_0$+N-EFIE$_I$	Dielectric

When the surface of D_u is a perfect electric conductor (PEC), the tangential component of the total electric field vanishes on the surface ($\boldsymbol{M} = 0$). Then, the scattering or radiation problem can be formulated and solved with T-EFIE, N-MFIE, T-MFIE, or N-MFIE, without using any combination. However, to avoid the internal resonance problem, it is necessary to combine EFIE and MFIE leading to a combined-field integral equation (CFIE) [20]. Specifically, a mixed formulation T-N-CFIE, which is obtained by the convex combination of T-EFIE and N-MFIE, is commonly used in the literature [3].

For scattering and radiation problems involving dielectric objects, integral equations are derived for both inner and outer media. These equations should be solved simultaneously to obtain $\boldsymbol{J}(\boldsymbol{r})$ and $\boldsymbol{M}(\boldsymbol{r})$. Similar to formulations of PEC objects, EFIE and MFIE can be combined in various ways to derive CFIE formulations, which are immune to the internal resonance problem. For example, TN-N-CFIE, which is obtained by combining T-EFIE, N-EFIE, and N-MFIE, was introduced for stable solutions [2]. On the other hand, many different formulations for dielectric objects are obtained by linearly combining the inner and outer equations while solving EFIE, MFIE, or their combinations simultaneously. For example, the tangential Poggio-Miller-Chang-Harrington-Wu-Tsai (T-PMCHWT) [1],[21],[22] formulation involves simultaneous solutions of T-EFIE and T-MFIE. A similar coupling of N-EFIE and N-MFIE leads to the well-known normal Müller formulation (NMF) [23]. Recently, these two formulations are improved by scaling EFIE and MFIE appropriately, leading to the combined tangential formulation (CTF) [13] and the modified normal Müller formulation (MNMF) [24], respectively. Although these formulations are free of the internal resonance problem, mixed formulations involving both tangential and normal equations are derived to obtain more stable solutions. For example, the electric and magnetic current combined-field integral equation (JMCFIE) [25], which involves all four equations, i.e., T-EFIE, N-EFIE, T-MFIE, and N-MFIE, provides fast iterative solutions, and it is preferable especially when the problem size is large [26]. Finally, electromagnetics problems involving composite dielectric-metallic structures can be formulated via hybrid formulations, which are obtained by applying different formulations for different parts of the objects [27]. Table I lists some of the surface formulations that are commonly used in the literature.

3. DISCRETIZATION

For numerical solutions, SIE formulations are discretized by using basis and testing functions. Equivalent currents are expanded in a series of basis functions $\boldsymbol{b}_n(\boldsymbol{r})$, i.e.,

$$\boldsymbol{J}(\boldsymbol{r}) = \sum_{n=1}^{N} \boldsymbol{x}[n]\boldsymbol{b}_n(\boldsymbol{r}) \tag{8}$$

$$\boldsymbol{M}(\boldsymbol{r}) = \sum_{n=1}^{N} \boldsymbol{y}[n]\boldsymbol{b}_n(\boldsymbol{r}), \tag{9}$$

where $\boldsymbol{x}$ and $\boldsymbol{y}$ are arrays of unknown coefficients. Testing the integral equations using a set of testing functions $\boldsymbol{t}_m(\boldsymbol{r})$, matrix equations are constructed and solved to calculate the unknown coefficients. Four basic matrix equations are derived as

$$\bar{\boldsymbol{T}}_u^T \cdot \boldsymbol{x} - \eta_u^{-1}\bar{\boldsymbol{K}}_u^T \cdot \boldsymbol{y} - \frac{1}{2}\eta_u^{-1}\bar{\boldsymbol{I}}^{\times n} \cdot \boldsymbol{y} = -\eta_u^{-1}\boldsymbol{v}_E \tag{10}$$

$$\bar{\boldsymbol{T}}_u^N \cdot \boldsymbol{x} - \eta_u^{-1}\bar{\boldsymbol{K}}_u^N \cdot \boldsymbol{y} + \frac{1}{2}\eta_u^{-1}\bar{\boldsymbol{I}} \cdot \boldsymbol{y} = -\eta_u^{-1}\boldsymbol{v}_E^{\times n} \tag{11}$$

$$\bar{\boldsymbol{T}}_u^T \cdot \boldsymbol{y} + \eta_u\bar{\boldsymbol{K}}_u^T \cdot \boldsymbol{x} + \frac{1}{2}\eta_u\bar{\boldsymbol{I}}^{\times n} \cdot \boldsymbol{x} = -\eta_u\boldsymbol{v}_H \tag{12}$$

$$\bar{\boldsymbol{T}}_u^N \cdot \boldsymbol{y} + \eta_u\bar{\boldsymbol{K}}_u^N \cdot \boldsymbol{x} - \frac{1}{2}\eta_u\bar{\boldsymbol{I}} \cdot \boldsymbol{x} = -\eta_u\boldsymbol{v}_H^{\times n}, \tag{13}$$

for T-EFIE, N-EFIE, T-MFIE, and N-MFIE, respectively. The interaction between the mth testing function $\boldsymbol{t}_m(\boldsymbol{r})$ and the nth basis function $\boldsymbol{b}_n(\boldsymbol{r})$ are calculated for different operators ($\mathcal{K}$, $\mathcal{T}$, and $\mathcal{I}$) and testing types (T and N) as

$$K_u^T[m,n] = \int_{S_m} d\boldsymbol{r}\boldsymbol{t}_m(\boldsymbol{r}) \cdot \int_{S_n,PV} d\boldsymbol{r'}\boldsymbol{b}_n(\boldsymbol{r'}) \times \nabla' g_u(\boldsymbol{r},\boldsymbol{r'}) \tag{14}$$

$$K_u^N[m,n] = \int_{S_m} d\boldsymbol{r}\boldsymbol{t}_m(\boldsymbol{r}) \cdot \hat{\boldsymbol{n}} \times \int_{S_n,PV} d\boldsymbol{r'}\boldsymbol{b}_n(\boldsymbol{r'}) \times \nabla' g_u(\boldsymbol{r},\boldsymbol{r'}) \tag{15}$$

$$\begin{aligned} T_u^T[m,n] = {} & ik_u \int_{S_m} d\boldsymbol{r}\boldsymbol{t}_m(\boldsymbol{r}) \cdot \int_{S_n} d\boldsymbol{r'}\boldsymbol{b}_n(\boldsymbol{r'}) g_u(\boldsymbol{r},\boldsymbol{r'}) \\ & - \frac{i}{k_u} \int_{S_m} d\boldsymbol{r}\boldsymbol{t}_m(\boldsymbol{r}) \cdot \int_{S_n} d\boldsymbol{r'}\nabla' \cdot \boldsymbol{b}_n(\boldsymbol{r'}) \nabla' g_u(\boldsymbol{r},\boldsymbol{r'}) \end{aligned} \tag{16}$$

$$\begin{aligned} T_u^N[m,n] = {} & ik_u \int_{S_m} d\boldsymbol{r}\boldsymbol{t}_m(\boldsymbol{r}) \cdot \hat{\boldsymbol{n}} \times \int_{S_n} d\boldsymbol{r'}\boldsymbol{b}_n(\boldsymbol{r'}) g_u(\boldsymbol{r},\boldsymbol{r'}) \\ & - \frac{i}{k_u} \int_{S_m} d\boldsymbol{r}\boldsymbol{t}_m(\boldsymbol{r}) \cdot \hat{\boldsymbol{n}} \times \int_{S_n} d\boldsymbol{r'}\nabla' \cdot \boldsymbol{b}_n(\boldsymbol{r'}) \nabla' g_u(\boldsymbol{r},\boldsymbol{r'}) \end{aligned} \tag{17}$$

$$I[m,n] = \int_{S_m} d\boldsymbol{r}\boldsymbol{t}_m(\boldsymbol{r}) \cdot \frac{\Omega_o(\boldsymbol{r})}{2\pi}\boldsymbol{b}_n(\boldsymbol{r}) \tag{18}$$

$$I^{\times n}[m,n] = \int_{S_m} d\boldsymbol{r}\boldsymbol{t}_m(\boldsymbol{r}) \cdot \hat{\boldsymbol{n}}\frac{\Omega_o(\boldsymbol{r})}{2\pi} \times \boldsymbol{b}_n(\boldsymbol{r}), \tag{19}$$

where S_m is the spatial support of the mth basis or testing function for $m = 1, 2, ..., N$. Elements of the right-hand-side (RHS) vectors in (10)–(13) are obtained by testing the incident electromagnetic fields, i.e.,

$$\boldsymbol{v}_E[m] = \int_{S_m} d\boldsymbol{r}\boldsymbol{t}_m(\boldsymbol{r}) \cdot \boldsymbol{E}^{inc}(\boldsymbol{r}) \tag{20}$$

$$\boldsymbol{v}_E^{\times n}[m] = \int_{S_m} d\boldsymbol{r}\boldsymbol{t}_m(\boldsymbol{r}) \cdot \hat{\boldsymbol{n}} \times \boldsymbol{E}^{inc}(\boldsymbol{r}) \tag{21}$$

$$\boldsymbol{v}_H[m] = \int_{S_m} d\boldsymbol{r}\boldsymbol{t}_m(\boldsymbol{r}) \cdot \boldsymbol{H}^{inc}(\boldsymbol{r}) \tag{22}$$

$$\boldsymbol{v}_H^{\times n}[m] = \int_{S_m} d\boldsymbol{r}\boldsymbol{t}_m(\boldsymbol{r}) \cdot \hat{\boldsymbol{n}} \times \boldsymbol{H}^{inc}(\boldsymbol{r}). \tag{23}$$

Using a Galerkin scheme and choosing the same set of functions as basis and testing functions, the

tangential equations, i.e., T-EFIE and T-MFIE, contain well-tested $\mathcal{T}$ operators, while the normal equations, i.e., N-EFIE and N-MFIE, contain well-tested $\mathcal{K}$ and $\mathcal{I}$ operators [2]. Then, tangential formulations involving T-EFIE and/or T-MFIE contain well-tested $\mathcal{T}$ operators, while normal formulations involving N-EFIE and/or N-MFIE contain well-tested $\mathcal{K}$ and $\mathcal{I}$ operators [13]. In mixed formulations, such as CFIE and JMCFIE, all kinds of operators are well-tested. In general, well-tested identity operators lead to well-conditioned matrix equations, which are easy to solve iteratively [28]. Therefore, for the efficiency of the solutions, normal and mixed formulations are preferable, especially when problems involve large objects discretized with large numbers of unknowns [26],[29],[30]. On the other hand, recent studies show that normal and mixed formulations are significantly inaccurate compared to tangential formulations [4]–[8], especially when they are discretized with low-order basis functions, such as RWG functions. Accuracy of normal and mixed formulations could be improved to the levels of tangential formulations by employing higher-order basis functions [13],[16],[17]. Investigations also show that the excessive error is caused by the well-tested identity operators [5],[18],[19]. In addition to the conditioning of the matrix equations, the identity operator seems to play a key role in the accuracy of the solutions via SIE formulations.

Using RWG functions on planar triangles, discretization of the well-tested identity operator is simple. The integral

$$I[m,n] = \int_{S_m} d\boldsymbol{r} \boldsymbol{t}_m(\boldsymbol{r}) \cdot \frac{\Omega_o(\boldsymbol{r})}{2\pi} \boldsymbol{b}_n(\boldsymbol{r}) = \int_{S_m} d\boldsymbol{r} \boldsymbol{t}_m(\boldsymbol{r}) \cdot \boldsymbol{b}_n(\boldsymbol{r}) \tag{24}$$

can be evaluated accurately by using a low-order Gaussian quadrature rule. On the other hand, the identity operator behaves like an operator with a highly-singular kernel [5],[18]. This alternative interpretation can be understood when (24) is rewritten as a double integral over the testing and basis functions as

$$I_{mn} = \int_{S_m} d\boldsymbol{r} \boldsymbol{t}_m(\boldsymbol{r}) \cdot \int_{S_n} d\boldsymbol{r'} \delta(\boldsymbol{r}, \boldsymbol{r'}) \boldsymbol{b}_n(\boldsymbol{r'}), \tag{25}$$

where $\delta(\boldsymbol{r}, \boldsymbol{r'})$ is a Dirac delta function representing a strong singularity. Consequently, the discretization of the identity operator may cause an unexpectedly large error, although its discretization involves very small or no error.

To demonstrate the inaccuracy of normal and mixed formulations compared to tangential formulations, we present the solution of electromagnetics problems involving canonical objects. Fig. 1 presents the results of a radiation problem involving a 1 cm $\times$ 1 cm $\times$ 1 cm PEC box located at the origin. As depicted in Fig. 1, the box is excited with a Hertzian dipole oriented in the z direction and located inside the box at $z = 0.35$ cm. Ideally, the radiated field outside the box should be zero due to the shielding provided by the closed PEC surface. We calculate the radiated field in the far zone on the x-y plane at $\boldsymbol{r} = (3 \text{ meters}, \pi/2, \phi_p)$, where $\phi_p = (p-1)\pi/180$ for $p = 1, 2, ..., 360$. The relative error is defined as the 2-norm of the total electric field divided by the 2-norm of the incident electric field, i.e.,

$$\Delta = \sqrt{\frac{\sum_{p=1}^{360} |E(3, \pi/2, \phi_p)|^2}{\sum_{p=1}^{360} |E^{inc}(3, \pi/2, \phi_p)|^2}} \qquad \Big(\phi_p = (p-1)\pi/180\Big). \tag{26}$$

The total electric field is obtained by adding the incident field due to the Hertzian dipole and the secondary field due to the induced electric current on the cube. Fig. 1 presents the relative error as a function of frequency from 20 GHz to 60 GHz. In this range of frequency, the size of the box varies from 0.67λ to 2λ. The radiation problem is discretized with 7200, 28,800, 115,200, and 460,800 unknowns, and solved by MLFMA without diagonalization [31]. We observe that T-N-CFIE $=$ $0.2 \times$ T-EFIE $+ 0.8 \times$ N-MFIE is significantly less accurate than T-EFIE. In order to obtain the same accuracy, the number of unknowns of T-N-CFIE should be 16 times larger than that of T-EFIE.

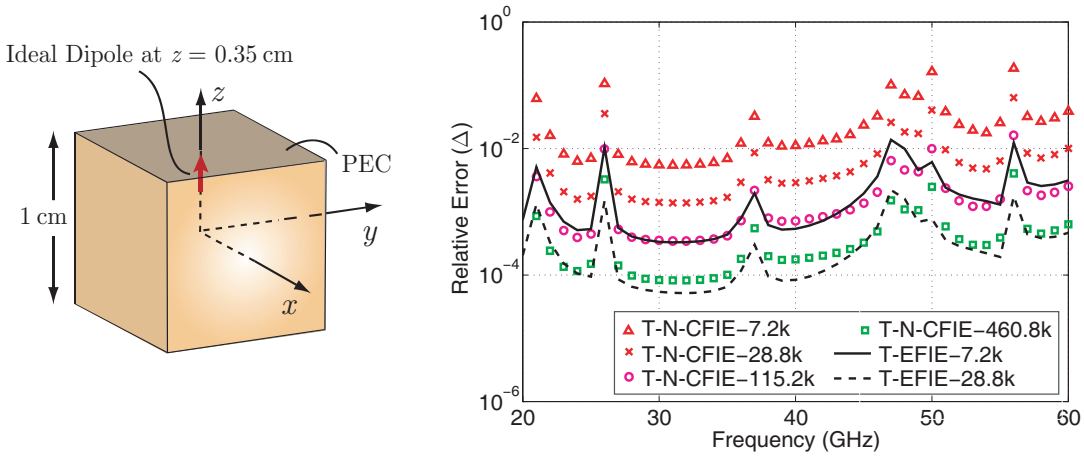

Fig. 1. Solutions of a radiation problem involving a 1 cm $\times$ 1 cm $\times$ 1 cm PEC box located at the origin and excited by a Hertzian dipole located inside the box at $z = 0.35$ cm. Relative error defined in (26) is plotted as a function of frequency from 20 GHz to 60 GHz.

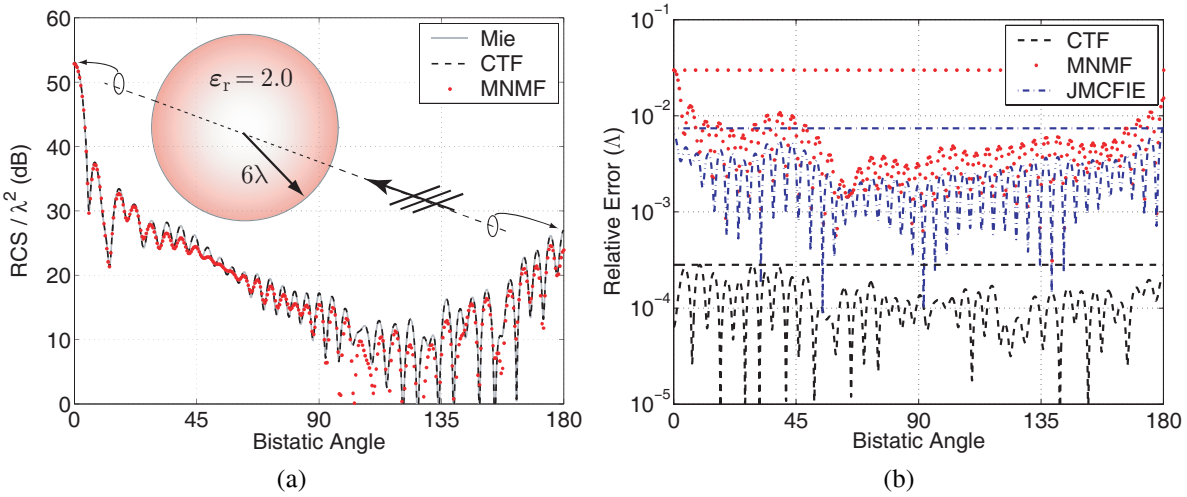

Fig. 2. Solutions of a scattering problem involving a dielectric sphere of radius 6λ illuminated by a plane wave. Relative permittivity of the sphere is 2.0 and it is located in free space. (a) Normalized bistatic RCS (RCS/λ^2) and (b) relative error defined in (27) for different formulations as a function of the bistatic angle.

Fig. 2 presents the solution of a scattering problem involving a dielectric sphere of radius 6λ, where λ is the wavelength outside the sphere (free space). The relative permittivity of the sphere is 2.0 and it is illuminated by a plane wave. The scattering problem is discretized with 264,006 unknowns and solved by MLFMA with three digits of accuracy. Fig. 2(a) presents the normalized radar cross section (RCS/λ^2 in dB) values on the E-plane as a function of the observation angle from 0° to 180°, where 0° corresponds to the forward-scattering direction. Computational values obtained with CTF and MNMF are compared with analytical values obtained by a Mie-series solution. We observe that the tangential formulation CTF provides more accurate results than the normal formulation MNMF. For more quantitative information, Fig. 2(b) presents the relative error in the computational results with respect to the reference analytical solution. In addition to CTF and MNMF, we also consider the error for the mixed formulation JMCFIE. The relative error as a function of bistatic angle φ is

defined as

$$\Lambda(\varphi) = \lim_{r\to\infty} \frac{|E_C^\infty(\varphi) - E_A^\infty(\varphi)|}{\max_\varphi |E_A^\infty(\varphi)|}, \tag{27}$$

where $E_C^\infty(\varphi)$ and $E_A^\infty(\varphi)$ are computational and analytical values of the far-zone electric field, i.e.,

$$E^\infty(\varphi) = \lim_{r\to\infty} rE(r,\varphi). \tag{28}$$

The maximum value of the relative error is also indicated by a horizontal line in the figure for each formulation. Fig. 2(b) shows that CTF provides the most accurate results, while MNMF is significantly inaccurate compared to CTF. Being a mixed formulation, accuracy of JMCIE is between CTF and MNMF.

4. EXCESSIVE DISCRETIZATION ERROR OF THE IDENTITY OPERATOR

In this section, we prove that the identity operator is truly a major error source, which contaminates the accuracy of SIE formulations. This is achieved by using the nonradiating property of the tangential incident fields on arbitrary surfaces [32],[33], i.e.,

$$\eta_u \mathcal{T}_u\{\boldsymbol{J}^{inc}\}(\boldsymbol{r}) - \mathcal{K}_u\{\boldsymbol{M}^{inc}\}(\boldsymbol{r}) + \frac{\Omega_i(\boldsymbol{r})}{4\pi}\mathcal{I}^{\times n}\{\boldsymbol{M}^{inc}\}(\boldsymbol{r}) = 0 \tag{29}$$

$$\frac{1}{\eta_u}\mathcal{T}_u\{\boldsymbol{M}^{inc}\}(\boldsymbol{r}) + \mathcal{K}_u\{\boldsymbol{J}^{inc}\}(\boldsymbol{r}) - \frac{\Omega_i(\boldsymbol{r})}{4\pi}\mathcal{I}^{\times n}\{\boldsymbol{J}^{inc}\}(\boldsymbol{r}) = 0, \tag{30}$$

where $\Omega_i(\boldsymbol{r})$ is the internal solid angle and $\{\boldsymbol{J}^{inc}(\boldsymbol{r}), \boldsymbol{M}^{inc}(\boldsymbol{r})\} = \{\hat{\boldsymbol{n}} \times \boldsymbol{H}^{inc}(\boldsymbol{r}), -\hat{\boldsymbol{n}} \times \boldsymbol{E}^{inc}(\boldsymbol{r})\}$. Nonradiating currents are expanded in a series of RWG functions, i.e.,

$$\boldsymbol{J}^{inc}(\boldsymbol{r}) = \sum_{n=1}^{N} \boldsymbol{x}^{inc}[n]\boldsymbol{b}_n(\boldsymbol{r}) \tag{31}$$

$$\boldsymbol{M}^{inc}(\boldsymbol{r}) = \sum_{n=1}^{N} \boldsymbol{y}^{inc}[n]\boldsymbol{b}_n(\boldsymbol{r}), \tag{32}$$

by using two methods. First, we consider an identity equation in the form of

$$\begin{bmatrix} \mathcal{I} & 0 \\ 0 & \mathcal{I} \end{bmatrix} \cdot \begin{bmatrix} \hat{\boldsymbol{n}} \times \boldsymbol{H}^{inc} \\ -\hat{\boldsymbol{n}} \times \boldsymbol{E}^{inc} \end{bmatrix} = \begin{bmatrix} \hat{\boldsymbol{n}} \times \boldsymbol{H}^{inc} \\ -\hat{\boldsymbol{n}} \times \boldsymbol{E}^{inc} \end{bmatrix}, \tag{33}$$

which can be discretized as

$$\begin{bmatrix} \bar{\boldsymbol{I}} & 0 \\ 0 & \bar{\boldsymbol{I}} \end{bmatrix} \cdot \begin{bmatrix} \boldsymbol{x}^{inc} \\ \boldsymbol{y}^{inc} \end{bmatrix} = \begin{bmatrix} \boldsymbol{v}_H^{\times n} \\ -\boldsymbol{v}_E^{\times n} \end{bmatrix}. \tag{34}$$

This method involves well-tested identity operators. The second method is based on the discretization of (29) and (30), i.e.,

$$\begin{bmatrix} \bar{\boldsymbol{T}}_u^T & -\eta_u^{-1}\bar{\boldsymbol{K}}_u^T \\ \eta_u\bar{\boldsymbol{K}}_u^T & \bar{\boldsymbol{T}}_u^T \end{bmatrix} \cdot \begin{bmatrix} \boldsymbol{x}^{inc} \\ \boldsymbol{y}^{inc} \end{bmatrix} = -\frac{1}{2}\begin{bmatrix} \eta_u^{-1}\boldsymbol{v}_E \\ \eta_u\boldsymbol{v}_H \end{bmatrix}, \tag{35}$$

which involves tangentially-tested $\mathcal{T}$ and $\mathcal{K}$ operators and does not contain any identity operator.

Fig. 3 presents the results of experiments involving a sphere of radius 0.5λ and a cube with edges of 0.5λ. Both objects are illuminated by a plane wave with unit amplitude. Nonradiating currents are expanded in a series of RWG functions on the objects using the two methods described above, i.e., using well-tested identity operators and using integro-differential $\mathcal{T}$ and $\mathcal{K}$ operators. Expansion coefficients are calculated and used to compute the radiated fields in the far zone on the E-plane. Fig. 3 presents the far-zone electric field, i.e., $E^\infty(\varphi)$ as a function of bistatic angle φ. Ideally, $\{\boldsymbol{J}^{inc}(\boldsymbol{r}), \boldsymbol{M}^{inc}(\boldsymbol{r})\}$ should not radiate and $E^\infty(\varphi)$ should be zero. Fig. 3(a) shows that the value

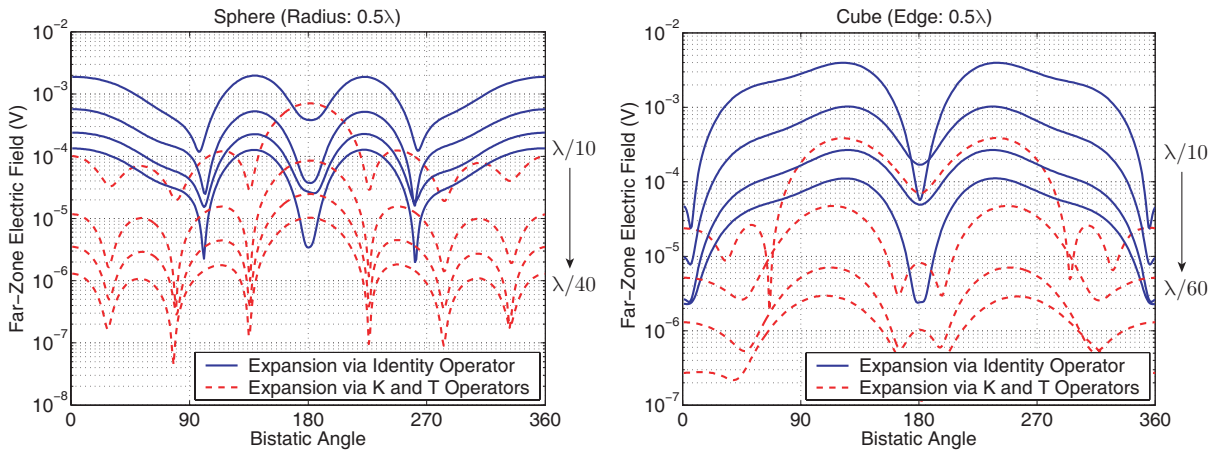

Fig. 3. Far-zone electric field due to nonradiating currents on (a) a sphere of radius 0.5λ and (b) a cube with edges of 0.5λ. Nonradiating currents discretized and expanded in a series of RWG functions by using two different methods involving well-tested identity operators and tangentially-tested integro-differential operators.

of $E^{\infty}(\varphi)$ drops as the mesh size decreases from $\lambda/10$ to $\lambda/40$ for the sphere. On the other hand, the two methods offer different levels of accuracy. Given a mesh size, error is smaller with the second method using the integro-differential operators, compared to the first method using well-tested identity operators. Fig. 3(b) presents similar results for the cube. The value of $E^{\infty}(\varphi)$ decreases as the triangulation becomes finer; but the first method generates larger error than the second method. We note that the first and second expansion methods are related to the solutions of electromagnetics problems with normal/mixed and tangential formulations, respectively, where the total currents (instead of nonradiating currents) are expanded in a series of basis functions.

5. CONTAMINATION OF THE ACCURACY OF SURFACE FORMULATIONS

Excessive discretization error of the identity operator contaminates the accuracy of normal and mixed formulations. Therefore, matrix equations obtained with tangential, normal, and mixed formulations for the same problem are incompatible. For example, consider the solution of an electromagnetics problems involving a closed PEC object. The problem can be formulated with T-EFIE and N-MFIE. Due to excessive discretization error of the identity operator in N-MFIE, solutions obtained with T-EFIE and N-MFIE are not equal, i.e.,

$$-\eta_u^{-1}\left\{\bar{\boldsymbol{T}}_u^T\right\}^{-1}\cdot\boldsymbol{v}_E=\boldsymbol{x}_E\neq\boldsymbol{x}_M=-\left\{\bar{\boldsymbol{K}}_u^N-0.5\bar{\boldsymbol{I}}\right\}^{-1}\cdot\boldsymbol{v}_H^{\times n}, \tag{36}$$

even when the solutions are free of internal resonances. We write

$$\boldsymbol{x}_M=\boldsymbol{x}_E+\Delta\boldsymbol{x}_{ME} \tag{37}$$

and the discrepancy between the solutions is interpreted as the error in N-MFIE. Consider the solution of the same problem with T-N-CFIE $=\alpha\times$ T-EFIE $+(1-\alpha)\times$ N-MFIE, i.e.,

$$\boldsymbol{x}_C=-\left\{\alpha\eta_u\bar{\boldsymbol{T}}_u^T+(1-\alpha)\left(\bar{\boldsymbol{K}}_u^N-0.5\bar{\boldsymbol{I}}\right)\right\}^{-1}\cdot\left\{\alpha\boldsymbol{v}_E+(1-\alpha)\boldsymbol{v}_H^{\times n}\right\}, \tag{38}$$

where $0 \leq \alpha \leq 1$. We note that

$$\begin{aligned}\boldsymbol{x}_C &= \Big\{\alpha\eta_u\bar{\boldsymbol{T}}_u^T + (1-\alpha)\big(\bar{\boldsymbol{K}}_u^N - 0.5\bar{\boldsymbol{I}}\big)\Big\}^{-1} \cdot \Big\{\alpha\eta_u\bar{\boldsymbol{T}}_u^T \cdot \boldsymbol{x}_E + (1-\alpha)\big(\bar{\boldsymbol{K}}_u^N - 0.5\bar{\boldsymbol{I}}\big) \cdot \boldsymbol{x}_M\Big\} \\ &= \Big\{\alpha\eta_u\bar{\boldsymbol{T}}_u^T + (1-\alpha)\big(\bar{\boldsymbol{K}}_u^N - 0.5\bar{\boldsymbol{I}}\big)\Big\}^{-1} \cdot \Big\{\alpha\eta_u\bar{\boldsymbol{T}}_u^T \cdot \boldsymbol{x}_E + (1-\alpha)\big(\bar{\boldsymbol{K}}_u^N - 0.5\bar{\boldsymbol{I}}\big) \cdot \boldsymbol{x}_E\Big\} \\ &+ \Big\{\alpha\eta_u\bar{\boldsymbol{T}}_u^T + (1-\alpha)\big(\bar{\boldsymbol{K}}_u^N - 0.5\bar{\boldsymbol{I}}\big)\Big\}^{-1} \cdot (1-\alpha)\big(\bar{\boldsymbol{K}}_u^N - 0.5\bar{\boldsymbol{I}}\big) \cdot (\boldsymbol{x}_M - \boldsymbol{x}_E) \\ &= \boldsymbol{x}_E + \Delta\boldsymbol{x}_{CE}, \end{aligned} \tag{39}$$

where

$$\Delta\boldsymbol{x}_{CE} = \Big\{\alpha\eta_u\bar{\boldsymbol{T}}_u^T + (1-\alpha)\big(\bar{\boldsymbol{K}}_u^N - 0.5\bar{\boldsymbol{I}}\big)\Big\}^{-1} \cdot (1-\alpha)\big(\bar{\boldsymbol{K}}_u^N - 0.5\bar{\boldsymbol{I}}\big) \cdot \Delta\boldsymbol{x}_{ME}. \tag{40}$$

Equations (39) and (40) describe how the T-N-CFIE solution is contaminated with the inaccuracy of N-MFIE due to the discretization error of the identity operator.

Consider an iterative solution of T-N-CFIE, where the residual error is minimized, i.e.,

$$\boldsymbol{r}_C = \alpha\boldsymbol{v}_E + (1-\alpha)\boldsymbol{v}_H^{\times n} + \Big\{\alpha\eta_u\bar{\boldsymbol{T}}_u^T + (1-\alpha)\big(\bar{\boldsymbol{K}}_u^N - 0.5\bar{\boldsymbol{I}}\big)\Big\} \cdot \tilde{\boldsymbol{x}}_C \to 0. \tag{41}$$

Rearranging the terms in (41), we obtain

$$\boldsymbol{r}_C = \alpha\boldsymbol{r}_{C\to E} + (1-\alpha)\boldsymbol{r}_{C\to M}, \tag{42}$$

where

$$\boldsymbol{r}_{C\to E} = \boldsymbol{v}_E + \eta_u\bar{\boldsymbol{T}}_u^T \cdot \tilde{\boldsymbol{x}}_C \tag{43}$$

$$\boldsymbol{r}_{C\to M} = \boldsymbol{v}_H^{\times n} + \big(\bar{\boldsymbol{K}}_u^N - 0.5\bar{\boldsymbol{I}}\big) \cdot \tilde{\boldsymbol{x}}_C \tag{44}$$

are residual vectors obtained by testing the T-N-CFIE solution in T-EFIE and N-MFIE systems, respectively. When the norm of $\boldsymbol{r}_C$ in (41) is minimized, norms of $\boldsymbol{r}_{C\to E}$ and $\boldsymbol{r}_{C\to M}$ are not necessarily minimized. Instead, $\boldsymbol{r}_{C\to E}$ and $\boldsymbol{r}_{C\to M}$ are scaled with respect to each other, i.e.,

$$\boldsymbol{r}_{C\to E} \approx -\frac{(1-\alpha)}{\alpha}\boldsymbol{r}_{C\to M}. \tag{45}$$

Then, an iterative solution of T-N-CFIE involves a breakpoint, where a further reduction of the residual error does not improve the compatibility of the solution with T-EFIE and N-MFIE. In general, iterative solutions of normal and mixed formulations discretized with low-order basis functions involve breakpoints, where the compatibility of the solution with the corresponding tangential formulation is saturated. More importantly, a breakpoint for the compatibility with the tangential formulation corresponds to the last useful iteration to obtain the highest possible accuracy with a normal or mixed formulation.

As an example, we consider the solution of a scattering problem involving a $\lambda \times \lambda \times \lambda$ PEC cube located at the origin. The cube is discretized with 2052 RWG functions and illuminated by a plane wave propagating in the $-x$ direction with the electric field polarized in the y direction. The scattering problem is solved with T-EFIE and T-N-CFIE ($\alpha = 0.2$) formulations. Matrix elements are calculated with a maximum of 1% error and solutions are performed iteratively by using the biconjugate-gradient-stabilized (BiCGStab) algorithm [34]. Fig. 4(a) presents the iterative solution of T-N-CFIE, where the 2-norm of the residual vector $\boldsymbol{r}_C$ is plotted with respect to BiCGStab iterations. We also plot the norms of $\boldsymbol{r}_{C\to E}$ and $\boldsymbol{r}_{C\to M}$ denoted by "T-N-CFIE to T-EFIE" and "T-N-CFIE to N-MFIE", respectively. The residual error is reduced to below 10^{-6} in 20 iterations. However, compatibility of the T-N-CFIE solution with the T-EFIE and N-MFIE systems is saturated at about 7th iterations. Fig. 4(b) presents both two solutions with T-EFIE and T-N-CFIE. Using T-EFIE, the residual error is reduced to below 10^{-6} in more than 300 iterations. In addition to residual errors, we calculate the error in the near-zone

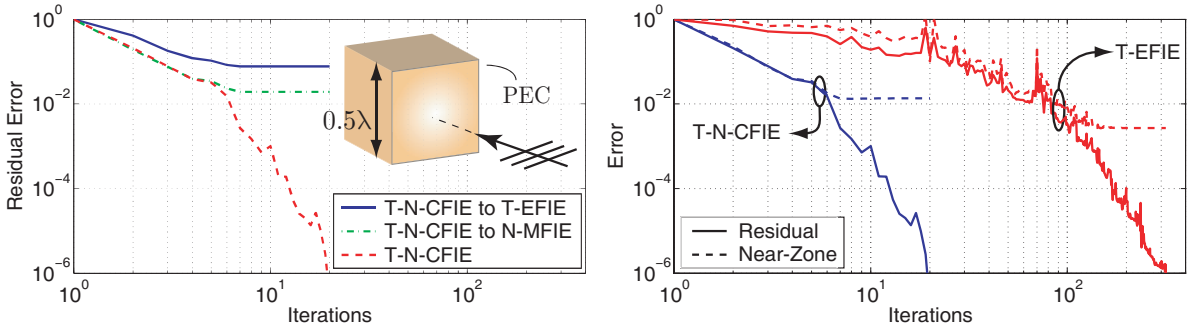

(a) (b)

Fig. 4. Iterative solutions of a scattering problem involving a $\lambda \times \lambda \times \lambda$ PEC cube illuminated by a plane wave propagating in the $-x$ direction with the electric field polarized in the y direction. (a) Residual errors with respect to iterations for T-N-CFIE. (b) Residual error and near-zone error defined in (46) with respect to iterations for T-N-CFIE and T-EFIE.

electric field at each iteration. The total electric field, which is obtained by combining the incident plane wave and the secondary field due to the induced electric current, is sampled inside the cube at $19 \times 19 = 361$ regularly-spaced points on the $z = 0$ plane. The total electric field should be zero inside the cube due to the shielding effect of the perfectly-conducting closed surface. Then, we define the near-zone error as

$$\Upsilon = \sqrt{\frac{\sum_{p=1}^{361} |E(x_p, y_p, 0)|^2}{\sum_{p=1}^{361} |E^{inc}(x_p, y_p, 0)|^2}} \qquad \Big(-\lambda/2 \leq x_p, y_p \leq \lambda/2 \Big). \tag{46}$$

As depicted in Fig. 4(b), the near-zone error in the T-EFIE solution is saturated at about 150th iteration, and the minimum achievable error is approximately 2.8×10^{-3}. Accuracy of the solution is saturated since there are various error sources, such as the numerical calculation of the matrix elements, and the overall error cannot be minimized by only reducing the residual error. In the T-N-CFIE solution, however, the minimum achievable error is directly related to the compatibility of the solution with the T-EFIE formulation. In this case, the near-zone error is saturated at 7th iteration, which corresponds to the breakpoint in Fig. 4(a), and the accuracy cannot be improved anymore. Consequently, a further reduction of the residual error is practically unnecessary.

6. CONCLUSION

In this study, we present our investigations on the contamination of SIE formulations with the excessive discretization error of the identity operator. Normal and mixed formulations involving well-tested identity operators are significantly inaccurate compared to tangential formulations, especially when they are discretized with low-order basis functions. By performing a computational experiment based on the nonradiating property of the tangential incident fields on arbitrary surfaces, we show that the identity operator is a major error source. Since normal and mixed formulations are contaminated with the excessive discretization error of the identity operator, matrix equations obtained with SIE formulations are incompatible. Then, minimization of the residual error during an iterative solution of a normal or mixed formulation involves a breakpoint, where the compatibility of the solution with the corresponding tangential formulation cannot be enhanced anymore. We show that the compatibility of a solution with a tangential formulation is an important indicator to determine the last useful iteration for the highest possible accuracy offered by SIE formulations.

REFERENCES

[1] A. J. Poggio and E. K. Miller, "Integral equation solutions of three-dimensional scattering problems," in *Computer Techniques for Electromagnetics*, R. Mittra, Ed. Oxford: Pergamon Press, 1973, Chap. 4.

[2] X.-Q. Sheng, J.-M. Jin, J. Song, W. C. Chew, and C.-C. Lu, "Solution of combined-field integral equation using multilevel fast multipole algorithm for scattering by homogeneous bodies," *IEEE Trans. Antennas Propagat.*, vol. 46, no. 11, pp. 1718–1726, Nov. 1998.

[3] J. Song, C.-C. Lu, and W. C. Chew, "Multilevel fast multipole algorithm for electromagnetic scattering by large complex objects," *IEEE Trans. Antennas Propagat.*, vol. 45, no. 10, pp. 1488–1493, Oct. 1997.

[4] Ö. Ergül and L. Gürel, "Investigation of the inaccuracy of the MFIE discretized with the RWG basis functions," in *Proc. IEEE Antennas and Propagation Soc. Int. Symp.*, vol. 3, 2004, pp. 3393–3396.

[5] C. P. Davis and K. F. Warnick, "High-order convergence with a low-order discretization of the 2-D MFIE," *IEEE Antennas Wireless Propagat. Lett.*, vol. 3, pp. 355–358, 2004.

[6] Ö. Ergül and L. Gürel, "Improved testing of the magnetic-field integral equation," *IEEE Microwave Wireless Comp. Lett.*, vol. 15, no. 10, pp. 615–617, Oct. 2005.

[7] Ö. Ergül and L. Gürel, "Solid-angle factor in the magnetic-field integral equation," *Microwave Opt. Technol. Lett.*, vol. 45, no. 5, pp. 452–456, June 2005.

[8] Ö. Ergül and L. Gürel, "On the accuracy of MFIE and CFIE in the solution of large electromagnetic scattering problems," in *Proc. European Conference on Antennas and Propagation (EuCAP)*, no. 350265, 2006.

[9] S. M. Rao, D. R. Wilton, and A. W. Glisson, "Electromagnetic scattering by surfaces of arbitrary shape," *IEEE Trans. Antennas Propagat.*, vol. AP-30, no. 3, pp. 409–418, May 1982.

[10] Ö. Ergül and L. Gürel, "Improving the accuracy of the MFIE with the choice of basis functions," in *Proc. IEEE Antennas and Propagation Soc. Int. Symp.*, vol. 3, 2004, pp. 3389–3392.

[11] E. Ubeda and J. M. Rius, "MFIE MOM-formulation with curl-conforming basis functions and accurate kernel integration in the analysis of perfectly conducting sharp-edged objects," *Microwave Opt. Technol. Lett.*, vol. 44, no. 4, pp. 354–358, Feb. 2005.

[12] E. Ubeda and J. M. Rius, "Monopolar divergence-conforming and curl-conforming low-order basis functions for the electromagnetic scattering analysis," *Microwave Opt. Technol. Lett.*, vol. 46, no. 3, pp. 237–241, Aug. 2005.

[13] P. Ylä-Oijala, M. Taskinen, and S. Järvenpää, "Surface integral equation formulations for solving electromagnetic scattering problems with iterative methods," *Radio Science*, vol. 40, RS6002, doi:10.1029/2004RS003169, Nov. 2005.

[14] E. Ubeda and J. M. Rius, "Novel monopolar MFIE MoM-discretization for the scattering analysis of small objects," *IEEE Trans. Antennas Propagat.*, vol. 54, no. 1, pp. 50–57, Jan. 2006.

[15] Ö. Ergül and L. Gürel, "The use of curl-conforming basis functions for the magnetic-field integral equation," *IEEE Trans. Antennas Propagat.*, vol. 54, no. 7, pp. 1917–1926, July 2006.

[16] Ö. Ergül and L. Gürel, "Improving the accuracy of the magnetic field integral equation with the linear-linear basis functions," *Radio Sci.*, vol. 41, RS4004, doi:10.1029/2005RS003307, July 2006.

[17] Ö. Ergül and L. Gürel, "Linear-linear basis functions for MLFMA solutions of magnetic-field and combined-field integral equations," *IEEE Trans. Antennas Propagat.*, vol. 55, no. 4, pp. 1103–1110, Apr. 2007.

[18] P. Ylä-Oijala, M. Taskinen, and S. Järvenpää, "Analysis of surface integral equations in electromagnetic scattering and radiation problems," *Engineering Analysis with Boundary Elements*, vol. 32, no. 3, pp. 196–209, Mar. 2008.

[19] K. F. Warnick and A. F. Peterson, "3D MFIE accuracy improvement using regularization," in *Proc. IEEE Antennas and Propagation Soc. Int. Symp.*, 2007, pp. 4857–4860.

[20] J. R. Mautz and R. F. Harrington, "H-field, E-field, and combined field solutions for conducting bodies of revolution," *AEÜ*, vol. 32, no. 4, pp. 157–164, Apr. 1978.

[21] T. K. Wu and L. L. Tsai, "Scattering from arbitrarily-shaped lossy dielectric bodies of revolution," *Radio Sci.*, vol. 12, pp. 709–718, Sep.-Oct. 1977.

[22] Y. Chang and R. F. Harrington, "A surface formulation for characteristic modes of material bodies," *IEEE Trans. Antennas Propagat.*, vol. AP-25, pp. 789–795, Nov. 1977.

[23] C. Müller, *Foundations of the Mathematical Theory of Electromagnetic Waves*. New York: Springer, 1969.

[24] P. Ylä-Oijala and M. Taskinen, "Well-conditioned Müller formulation for electromagnetic scattering by dielectric objects," *IEEE Trans. Antennas Propagat.*, vol. 53, no. 10, pp. 3316–3323, Oct. 2005.

[25] P. Ylä-Oijala and M. Taskinen, "Application of combined field integral equation for electromagnetic scattering by dielectric and composite objects," *IEEE Trans. Antennas Propagat.*, vol. 53, no. 3, pp. 1168–1173, Mar. 2005.

[26] Ö. Ergül and L. Gürel, "Comparison of integral-equation formulations for the fast and accurate solution of scattering problems involving dielectric objects with the multilevel fast multipole algorithm," *IEEE Trans. Antennas Propagat.*, accepted for publication.

[27] P. Ylä-Oijala, M. Taskinen, and J. Sarvas, "Surface integral equation method for general integral equation method for general composite metallic and dielectric structures with junctions," *Progress In Electromagnetics Research (PIER)*, vol. 52, pp. 81-108, doi:10.2528/PIER04071301, 2005.

[28] D. R. Wilton and J. E. Wheeler III, "Comparison of convergence rates of the conjugate gradient method applied to various integral equation formulations," *Progress in Electromagnetics Research PIER 05*, pp. 131–158, 1991.

[29] L. Gürel and Ö. Ergül, "Comparisons of FMM implementations employing different formulations and iterative solvers," in *Proc. IEEE Antennas and Propagation Soc. Int. Symp.*, vol. 1, 2003, pp. 19–22.

[30] L. Gürel and Ö. Ergül, "Fast and accurate solutions of integral-equation formulations discretised with tens of millions of unknowns," *Electronics Lett.*, vol. 43, no. 9, pp. 499–500, Apr. 2007.

[31] L. J. Jiang and W. C. Chew, "A mixed-form fast multipole algorithm," *IEEE Trans. Antennas Propagat.*, vol. 53, no. 12, pp. 4145–4156, Dec. 2005.

[32] G. C. Hsiao and R. E. Kleinman, "Mathematical foundations for error estimation in numerical solutions of integral equations in electromagnetics," *IEEE Trans. Antennas Propagat.*, vol. 45, no. 3, pp. 316–328, Mar. 1997.

[33] Ö. Ergül and L. Gürel, "Stabilization of integral-equation formulations for the accurate solution of scattering problems involving low-contrast dielectric objects," *IEEE Trans. Antennas Propagat.*, vol. 56, no. 3, pp. 799–805, Mar. 2008.

[34] H. A. van der Vorst, "Bi-CGSTAB: A fast and smoothly converging variant of Bi-CG for the solution of nonsymmetric linear systems," *SIAM J. Sci. Statist. Comput.*, vol. 13, no. 2, pp. 631–644, Mar. 1992.